Title

On the Green's function of the partially diffusion-controlled reversible ABCD reaction for radiation chemistry codes

Authors' names

Ianik Plante[*†§], Luc Devroye[‡]

Authors' affiliations

[*]Wyle Science, Technology & Engineering
1290 Hercules, Houston, TX 77058

[†]NASA Johnson Space Center
Bldg 37, Mail Code SK
2101 NASA Parkway, Houston, TX 77058

[‡]School of Computer Science
McGill University
3480 University Street, Montreal H3A 0E9 (Canada)

Email: ianik.plante-1@nasa.gov
lucdevroye@gmail.com

[§]Corresponding Author:

Ianik Plante
NASA Johnson Space Center
2101 NASA Parkway
Mail Code SK
Houston TX 77058
Office: 281 483-0968
Fax: 281 483-3058

TITLE RUNNING HEAD

Radiation chemistry based Green's functions

Receipt date

April 30, 2015

Abstract

Several computer codes simulating chemical reactions in particles systems are based on the Green's functions of the diffusion equation (GFDE). Indeed, many types of chemical systems have been simulated using the exact GFDE, which has also become the gold standard for validating other theoretical models. In this work, a simulation algorithm is presented to sample the interparticle distance for partially diffusion-controlled reversible ABCD reaction. This algorithm is considered exact for 2-particles systems, is faster than conventional look-up tables and uses virtually no memory. The simulation results obtained with this method are compared with those obtained with the independent reaction times (IRT) method. This work is part of our effort in developing models to understand the role of chemical reactions in the radiation effects of human body and may eventually be included in event-based models of space radiation risks. However, as many reactions are of this type in biological systems, this algorithm might play a pivotal role in future simulation programs not only in radiation chemistry, but also in the simulation of biochemical networks in time and space as well.

Physics and Astronomy Classification Scheme (PACS) indexing codes

87.15.A- Theory, modeling, and computer simulation
87.15.ak Monte Carlo simulations
82.37.Np Single molecule reaction kinetics, dissociation, etc.
87.53.Ay Biophysical mechanisms of interaction

1. Introduction

Simulations based on the Green's functions of the diffusion equation (GFDE) have been widely used to the study chemical reactions in solutions [1-13]. More recently, this approach has been used in radiation chemistry codes to simulate the radiolysis of water and aqueous solutions [14-15], chemical dosimeters [16] and to study of interaction of ligand molecules with receptors [17]. In the radiolysis of water and aqueous solutions of interest for biological systems, most reactions are diffusion-controlled and partially diffusion-controlled. In radiation chemistry codes, the algorithms usually simulate forward reactions, and the possibility of the backward reaction is taken into account by considering the reaction of the products as a forward reaction. In other words, the forward and backward components of reversible reactions are treated separately.

In previous work, we have developed exact random number generators to simulate the reversible partially diffusion-controlled ABC reaction[1], considering the forward and backward reactions together [18]. In this paper, the method is extended to the simulation of the reversible partially diffusion-controlled ABCD reaction. The structure of this paper is as follows. In the first part, the GFDE and the peculiarities for this particular system are presented. This GFDE is considered exact for an isolated pair of particles with partially diffusion-controlled ABCD reaction and, therefore, might play a pivotal role in development and validation of models comprising many particles. In the second part, we present an exact sampling algorithm based on the rejection method for the Green's functions. In the third part, simulation results are presented, and compared with those obtained with the independent reaction times (IRT) method. The performance and precision of the algorithm are compared with standard look-up table methods commonly used for this type of calculation. The algorithms will eventually be used in Brownian Dynamics codes to

[1] The reversible ABC reaction is $A + B \underset{k_2}{\overset{k_1}{\rightleftarrows}} C$

simulate the radiation chemistry of the radiolytic species (such as the free radical ·OH) created by the interaction of ionizing radiation with water and to study DNA damage by the indirect effect.

2. The GFDE for reversible partially diffusion-controlled ABCD reactions

2.1 General considerations

The reversible partially diffusion-controlled ABCD reaction can be written

$$A + B \underset{k_2}{\overset{k_1}{\rightleftarrows}} C + D, \tag{1}$$

where k_1 and k_2 are the rate constants for the forward and reverse reaction, respectively. The units of k_1 and k_2 are $[length]^3[time]^{-1}$. As it is well known [8-9], the probability distribution function of a pair of particles such as $p(\boldsymbol{x_A}, \boldsymbol{x_B}, t|\boldsymbol{x_{A_0}}, \boldsymbol{x_{B_0}})$ where $\boldsymbol{x_A}$, $\boldsymbol{x_B}$, $\boldsymbol{x_{A_0}}$and $\boldsymbol{x_{B_0}}$ are the position vectors of the particles at time t and $t=0$, respectively, can be factored as $p(\boldsymbol{x},t|\boldsymbol{x_0})p(\boldsymbol{X},t|\boldsymbol{X_0})$, by using the transformation

$$\boldsymbol{X} = \sqrt{D_B/D_A}\boldsymbol{x_A} + \sqrt{D_A/D_B}\boldsymbol{x_B}, \tag{2a}$$
$$\boldsymbol{x} = \boldsymbol{x_B} - \boldsymbol{x_A}. \tag{2b}$$

Here D_A and D_B are the diffusion coefficients of particles A and B, $\boldsymbol{x}$ and $\boldsymbol{x_0}$ are the relative position vectors, and $\boldsymbol{X}$ and $\boldsymbol{X_0}$ are the position vectors of the "center of mass". This factorization yields two diffusion equations, one for the center of mass and one for the relative position vector. This proof is not repeated here but we bear in mind that the GFDE provided in the following section represent relative position vectors, and that the center of mass diffusion will not be considered. The angular dependency of the GFDE will not be considered.

2.2 Green's functions for the partially diffusion-controlled ABCD reactions

In a two-particle system, the particles can be either in the form AB or CD at time t. In this paper, the notation x_i is used for the inter-particle distance for pairs in the form AB, and y_i is used for particles in the form CD. We now define the Green's functions $p_1(x_1,t|x_0)$, $p_2(y_1,t|x_0)$, $p_3(y_1,t|y_0)$, and $p_4(x_1,t|y_0)$, which

yield the probabilities that the inter-particle distance at time t will be x_1 or y_1, given that it was initially x_0 or y_0. They are solutions of the following diffusion equations:

$$\frac{\partial p_1(x_1,t\,|\,x_0)}{\partial t}=\frac{D_1}{x_1^2}\frac{\partial}{\partial x_1}\left(x_1^2\frac{\partial}{\partial x_1}p_1(x_1,t\,|\,x_0)\right);\ \frac{\partial p_2(y_1,t\,|\,x_0)}{\partial t}=\frac{D_2}{y_1^2}\frac{\partial}{\partial y_1}\left(y_1^2\frac{\partial}{\partial y_1}p_2(y_1,t\,|\,x_0)\right); \quad (3a)$$

$$\frac{\partial p_3(y_1,t\,|\,y_0)}{\partial t}=\frac{D_2}{y_1^2}\frac{\partial}{\partial y_1}\left(y_1^2\frac{\partial}{\partial y_1}p_3(y_1,t\,|\,y_0)\right);\ \frac{\partial p_4(x_1,t\,|\,y_0)}{\partial t}=\frac{D_1}{x_1^2}\frac{\partial}{\partial x_1}\left(x_1^2\frac{\partial}{\partial x_1}p_4(x_1,t\,|\,y_0)\right); \quad (3b)$$

where $D_1=D_A+D_B$ and $D_2=D_C+D_D$ are the sum of the diffusion coefficients of particles. For a pair of particles in the initial state AB at separation distance x_0, the initial conditions are:

$$4\pi x_0^2\,p_1(x,t=0\,|\,x_0)=\delta(\mathrm{x}-\mathrm{x}_0),\ p_2(y,t=0\,|\,x_0)=0. \quad (4a)$$

$$4\pi y_0^2\,p_3(y,t=0\,|\,y_0)=\delta(\mathrm{y}-\mathrm{y}_0),\ p_4(x,t=0\,|\,y_0)=0. \quad (4b)$$

The boundary conditions can be written

$$4\pi a_1^2 D_1\left.\frac{\partial p_1(x_1,t\,|\,x_0)}{\partial x_1}\right|_{x_1=a_1}=-4\pi a_2^2 D_2\left.\frac{\partial p_2(y_1,t\,|\,x_0)}{\partial y_1}\right|_{y_1=a_2}=k_1p_1(a_1,t\,|\,x_0)-k_2p_2(a_2,t\,|\,x_0), \quad (5a)$$

$$4\pi a_2^2 D_2\left.\frac{\partial p_3(y_1,t\,|\,y_0)}{\partial y_1}\right|_{y_1=a_2}=-4\pi a_1^2 D_1\left.\frac{\partial p_4(x_1,t\,|\,y_0)}{\partial x_1}\right|_{x_1=a_1}=k_2p_3(a_2,t\,|\,y_0)-k_1p_4(a_1,t\,|\,y_0), \quad (5b)$$

where a_1 and a_2 are the reaction radii for the forward and backward reactions, The equations are similar to the familiar boundary conditions for partially diffusion-controlled reactions, with an added term for the contribution of the backward reaction.

It is useful at this point to introduce the functions *Erfc(x)*, *W(x,y)* and *Ω(x)*:

$$Erfc(x)=\frac{2}{\sqrt{\pi}}\int_x^\infty\exp(-\xi^2)d\xi, \quad (6a)$$

$$W(x,y)=\exp(2xy+y^2)Erfc(x+y), \quad (6b)$$

$$\Omega(x)=\exp(x^2)Erfc(x). \quad (6c)$$

The following analytical expressions are simplified by using the notation

$$\chi_i=(x_i-a_1)/\sqrt{4D_1t}, \quad (7a)$$

$$\gamma_i=(y_i-a_2)/\sqrt{4D_2t}. \quad (7b)$$

We also define the diffusion control rate constant $k_{D_i}\equiv 4\pi D_i a_i$ and time scale $\tau_i\equiv a_i^2/D_i$. Furthermore, we define $\sigma_\pm$, μ_i and λ:

$$\sigma_\pm=\frac{1}{2}\left[\mu_1+\mu_2\pm\sqrt{(\mu_1-\mu_2)^2+\lambda}\right], \quad (8a)$$

$$\mu_i = (1 + k_i / k_{D_i}) / \sqrt{\tau_i}\ , \tag{8b}$$

$$\lambda = \frac{4k_1k_2}{k_{D_1}k_{D_2}\sqrt{\tau_1\tau_2}}\,. \tag{8c}$$

The Green's functions for the pair initially in the AB form with inter-particle distance x_0 are [1, 10]:

$$\begin{aligned} p_1(x_1,t\,|\,x_0) = \mathrm{p}_{\mathrm{ref}_1}(x_1,t\,|\,x_0) - \frac{k_1a_1^2}{\sqrt{\tau_1\tau_2}k_{D_1}^2x_1x_0}\Bigg[\frac{\sigma_+}{\sigma_+-\sigma_-}\frac{1-\sigma_+\sqrt{\tau_2}}{1-\sigma_+\sqrt{\tau_1}}W\left(\chi_1+\chi_0,\sigma_+\sqrt{t}\right) \\ -\frac{\sigma_-}{\sigma_+-\sigma_-}\frac{1-\sigma_-\sqrt{\tau_2}}{1-\sigma_-\sqrt{\tau_1}}W\left(\chi_1+\chi_0,\sigma_-\sqrt{t}\right)-\left(1-\sqrt{\frac{\tau_2}{\tau_1}}\right)\frac{W(\chi_1+\chi_0,\sigma_+\sqrt{t/\tau_1})}{(1-\sigma_+\sqrt{\tau_1})(1-\sigma_-\sqrt{\tau_1})}\Bigg]\end{aligned}, \tag{9}$$

$$p_2(y_1,t\,|\,x_0) = \frac{k_1a_1a_2}{\sqrt{\tau_1\tau_2}k_{D_1}k_{D_2}y_1x_0(\sigma_+-\sigma_-)}\left[\sigma_+W\left(\chi_0+\gamma_1,\sigma_+\sqrt{t}\right)-\sigma_-W\left(\chi_0+\gamma_1,\sigma_-\sqrt{t}\right)\right]. \tag{10}$$

The Green's functions for the pair initially in the CD form are obtained by interchanging the appropriate constants in the corresponding Green's functions in the AB form.

$$\begin{aligned} p_3(y_1,t\,|\,y_0) = \mathrm{p}_{\mathrm{ref}_2}(y_1,t\,|\,y_0) - \frac{k_2a_2^2}{\sqrt{\tau_1\tau_2}k_{D_2}^2y_1y_0}\Bigg[\frac{\sigma_+}{\sigma_+-\sigma_-}\frac{1-\sigma_+\sqrt{\tau_1}}{1-\sigma_+\sqrt{\tau_2}}W\left(\gamma_1+\gamma_0,\sigma_+\sqrt{t}\right) \\ -\frac{\sigma_-}{\sigma_+-\sigma_-}\frac{1-\sigma_-\sqrt{\tau_1}}{1-\sigma_-\sqrt{\tau_2}}W\left(\gamma_1+\gamma_0,\sigma_-\sqrt{t}\right)-\left(1-\sqrt{\frac{\tau_1}{\tau_2}}\right)\frac{W(\gamma_1+\gamma_0,\sigma_+\sqrt{t/\tau_2})}{(1-\sigma_+\sqrt{\tau_2})(1-\sigma_-\sqrt{\tau_2})}\Bigg]\end{aligned}, \tag{11}$$

$$p_4(x_1,t\,|\,y_0) = \frac{k_2a_1a_2}{\sqrt{\tau_1\tau_2}k_{D_1}k_{D_2}x_1y_0(\sigma_+-\sigma_-)}\left[\sigma_+W\left(\chi_1+\gamma_0,\sigma_+\sqrt{t}\right)-\sigma_-W\left(\chi_1+\gamma_0,\sigma_-\sqrt{t}\right)\right]. \tag{12}$$

In Eqs. 9 and 11, $\mathrm{p}_{\mathrm{ref}_1}(x_1,t\,|\,x_0)$ and $\mathrm{p}_{\mathrm{ref}_2}(y_1,t\,|\,y_0)$ are the well-known Green's function for free diffusion with a reflective boundary condition

$$\mathrm{p}_{\mathrm{ref}_1}(x_1,t\,|\,x_0) = \frac{1}{4\pi x_1x_0a_1}\left[\sqrt{\frac{\tau_1}{4\pi t}}\left(e^{-(\chi_1-\chi_0)^2}+e^{-(\chi_1+\chi_0)^2}\right)-W\left(\chi_1+\chi_0,\sqrt{\frac{t}{\tau_1}}\right)\right], \tag{13a}$$

$$\mathrm{p}_{\mathrm{ref}_2}(y_1,t\,|\,y_0) = \frac{1}{4\pi y_1y_0a_2}\left[\sqrt{\frac{\tau_2}{4\pi t}}\left(e^{-(\gamma_1-\gamma_0)^2}+e^{-(\gamma_1-\gamma_0)^2}\right)-W\left(\gamma_1+\gamma_0,\sqrt{\frac{t}{\tau_2}}\right)\right]. \tag{13b}$$

The reaction probabilities can be obtained by integration of the Green's functions over all possible exit points after reaction, i.e. $x_1 \geq a_1$ and $y_1 \geq a_2$. As there are potentially numerous forward and backward reactions during the time interval t, the integration results are interpreted as effective reaction probabilities. The calculation for the effective forward reaction probability yields:

$$P_{AB\to CD}(t\,|\,x_0)=\int_{a_2}^{\infty} p_2(y_1,t\,|\,x_0)\,4\pi y_1^2\,dy_1=\frac{a_1}{x_0}\frac{k_1/k_{D_1}}{1+k_1/k_{D_1}+k_2/k_{D_2}}\left[Erfc\chi_0+\frac{\sigma_-(1-\sigma_+\sqrt{\tau_2})}{\sigma_+-\sigma_-}W\left(\chi_0,\sigma_+\sqrt{t}\right)-\frac{\sigma_+(1-\sigma_-\sqrt{\tau_2})}{\sigma_+-\sigma_-}W\left(\chi_0,\sigma_-\sqrt{t}\right)\right]. \quad (14)$$

For the effective backward reaction probability, the result is:

$$P_{CD\to AB}(t\,|\,y_0)=\int_{a_1}^{\infty} p_4(x_1,v\,|\,y_0)\,4\pi x_1^2\,dx_1=\frac{a_2}{y_0}\frac{k_2/k_{D_2}}{1+k_1/k_{D_1}+k_2/k_{D_2}}\left[Erfc\gamma_0+\frac{\sigma_-(1-\sigma_+\sqrt{\tau_1})}{\sigma_+-\sigma_-}W\left(\gamma_0,\sigma_+\sqrt{t}\right)-\frac{\sigma_+(1-\sigma_-\sqrt{\tau_1})}{\sigma_+-\sigma_-}W\left(\gamma_0,\sigma_-\sqrt{t}\right)\right]. \quad (15)$$

When $\tau_1=\tau_2=\tau$, $\sqrt{\tau}\sigma_-=1$ and $\sqrt{\tau}\sigma_+=1+k_1/k_{D_1}+k_2/k_{D_2}$, there is a division by 0 in $p_1(x_1,t|x_0)$ and in $p_3(y_1,t|y_0)$. However, it is still possible to evaluate $p_1(x_1,t|x_0)$ and $p_3(y_1,t|y_0)$ by using the limit $\tau_2\to\tau_1$. A short calculation yields (see Mathematica supporting document):

$$\lim_{\tau_2\to\tau_1} p_1(x_1,t\,|\,x_0)=\mathrm{p}_{\mathrm{ref}_1}(x_1,t\,|\,x_0)-\frac{k_1a_1^2}{k_{D_1}^2x_1x_0\tau(\sigma_+-\sigma_-)}\left[\sigma_+W\left(\chi_1+\chi_0,\sigma_+\sqrt{t}\right)-\sigma_-W\left(\chi_1+\chi_0,\sigma_-\sqrt{t}\right)\right], \quad (16a)$$

$$\lim_{\tau_2\to\tau_1} p_3(y_1,t\,|\,y_0)=\mathrm{p}_{\mathrm{ref}_2}(y_1,t\,|\,y_0)-\frac{k_2a_2^2}{k_{D_2}^2y_1y_0\tau(\sigma_+-\sigma_-)}\left[\sigma_+W\left(\gamma_1+\gamma_0,\sigma_+\sqrt{t}\right)-\sigma_-W\left(\gamma_1+\gamma_0,\sigma_-\sqrt{t}\right)\right]. \quad (16b)$$

2.3 Time discretization equations

A simulation is usually done in several time steps. Therefore, if a given 2-particle system with specified initial conditions is simulated many times, the number of pairs in the states AB and CD, as well as the distribution of distances of the pair at the end of the simulation, should only depend on the sum of the time steps. This follows from the properties of Markov processes.

In Appendix A, we show that the Green's functions for a system with specified initial conditions only depends of the sum of the time steps. This property was used to validate the simulation algorithms. For example, consider a pair AB initially at distance x_0. After one time step (Δt_1), the values of x_1 are distributed as $p_1(x_1,\Delta t_1|x_0)$. These values of x_1 become the initial values for the next time step (Δt_2). But according to the theory we know that the values of x_2 sampled after the second time step (Δt_2) will be distributed as $p_1(x_2,\Delta t_1+\Delta t_2|x_0)$. Since the sampling algorithm in the second time step is used with various initial values x_1, the algorithm is verified simultaneously for a whole range of the parameter x_1. The property also allows the verification of the algorithm for the interparticle distance distribution in the CD

state, as the distribution of y_2 after two time steps comprises the contribution of the forward and backward reactions.

3. Methods

3.1 Algorithms for simulating the Green's functions of the ABCD reactions

In a previous paper [18], we have developed an algorithm to sample the GFDE for the reversible partially diffusion-controlled ABC reaction. Since the Green's functions for the ABCD reactions are similar to those for the ABC reactions, it is possible to adapt the algorithms to sample the Green's functions for the ABCD reaction.

3.1.1 Sampling of the Green's function with a reflective boundary

As it was the case for the propagator for the reaction ABC, the function $4\pi x_1^2 p_1(x_1, t|x_0)$ is a sub-density[2] of $f_1(x_1) = 4\pi x_1^2 p_{ref_1}(x_1, t|x_0)$. Therefore, we will briefly recall the algorithm to generate random variates[3] for non-reacting particles. The distribution to sample is

$$f_1(x_1) = \frac{x_1}{x_0\sqrt{4\pi D_1 t}}\left\{\exp\left[-\frac{(x_1-x_0)^2}{4D_1 t}\right] + \exp\left[-\frac{(x_1+x_0-2a_1)^2}{4D_1 t}\right] - \frac{\sqrt{4\pi D_1 t}}{a_1} W\left(\frac{x_1+x_0-2a_1}{\sqrt{4D_1 t}}, \frac{\sqrt{D_1 t}}{a_1}\right)\right\}, \; x_1 > a_1. \tag{17}$$

This distribution is normalized, i.e.:

$$\int_{a_1}^{\infty} f_1(x_1)dx_1 = 1. \tag{18}$$

The objective is to generate random variates X_1 from $f_1(x_1)$. This probability distribution is univariate, but includes four parameters x_0, a_1, D_1 and t. As previously shown, $f_1(x_1)$ can be written as a two-parameter

---

[2] In general, a sub-density means that $\int f(x)dx = P$, where 0<P<1. In the context of this article, P is the probability of the pair to remain in the state AB during the time step. In this case, a random variate with density f/P can be generated with probability P.

[3] The terminology given in the book of Devroye [20] for non-uniform random variate generation will be used here.

distribution. However, to avoid introducing more variables, the algorithm is given here in its original form.

Since $W \geq 0$, it is clear that $f_1(x_1) \leq h(x_1)$, where

$$h(x_1) = \frac{x_1}{x_0\sqrt{4\pi D_1 t}}\left\{\exp\left[-\frac{(x_1 - x_0)^2}{4D_1 t}\right] + \exp\left[-\frac{(x_1 + x_0 - 2a_1)^2}{4D_1 t}\right]\right\}, \; x_1 \geq a_1. \tag{19}$$

Therefore, von Neumann's rejection method [20-21] can be used. The rejection method is a well-known general sampling technique to generate random variates of a probability distribution $p(x)$, which does not require that the cumulative distribution function (the indefinite integral of $p(x)$) be computable. To use this technique, we assume that $p(x) \leq Cg(x)$, where C is a proportionality constant such as $C \geq 1$ and $g(x)$ is a probability distribution for which random variates X distributed as $g(x)$ can be easily generated. To generate random variates distributed as $p(x)$, a uniformly distributed random number U between 0 and 1 and a random variate X distributed as $g(x)$ are generated. The value of X is accepted if the condition $UCg(X) \leq p(X)$ is verified; otherwise, a new set of U and X are generated until the condition is true. From a geometric perspective, points are generated in the 2D plane bounded by the curve $Cg(x)$ and the domain of $g(x)$; the points that are accepted are those which fall under $p(x)$.

In the actual problem, since $f_1(x_1)$ is bounded from above by the first two terms ($h(x_1)$), the third (negative) term is ignored at this moment. The function $h(x_1)$ can be written as the sum of four terms $h_i(x_1)$, i=1..4, and truncated to the positive ranges as follows:

$$h_1(x_1) = \frac{x_1 - x_0}{x_0\sqrt{4\pi D_1 t}}\exp\left[-\frac{(x_1 - x_0)^2}{4D_1 t}\right] \times \mathbf{1}_{[x_1 \geq x_0]}. \tag{20a}$$

$$h_2(x_1) = \frac{x_1 + x_0 - 2a_1}{x_0\sqrt{4\pi D_1 t}}\exp\left[-\frac{(x_1 + x_0 - 2a_1)^2}{4D_1 t}\right] \times \mathbf{1}_{[x_1 \geq a_1]}. \tag{20b}$$

$$h_3(x_1) = \frac{x_0}{x_0\sqrt{4\pi D_1 t}}\exp\left[-\frac{(x_1 - x_0)^2}{4D_1 t}\right] \times \mathbf{1}_{[x_1 \geq a_1]}. \tag{20c}$$

$$h_4(x_1) = \frac{2a_1 - x_0}{x_0\sqrt{4\pi D_1 t}} \exp\left[-\frac{(x_1 + x_0 - 2a_1)^2}{4D_1 t}\right] \times \mathbf{1}_{[x_1 \geq a_1]} \times \mathbf{1}_{[x_0 \leq 2a_1]}. \quad (20d)$$

where $\mathbf{1}_{[\text{condition}]}$ takes the value 1 when the condition is true, and 0 when it is false. The first exponential of Eq. 19 is $\leq(h_1+h_3)$, because $x_1 \leq (x_1-x_0)_+ + x_0$, where the subscript + indicates the positive part. Similarly, the second exponential of Eq. 19 is $\leq(h_2+h_4)$, because $x_1 \leq (x_1-(2a_1-x_0))_+ + (2a_1-x_0)_+$. Since $x_0 \geq a_1$ and $x_1 \geq a_1$, it follows that $x_0+x_1 \geq 2a_1$, so that $x_1 \leq (x_1-(2a_1-x_0)) + (2a_1-x_0)_+$.

Since $f_1(x_1) \leq h_{tr}(x_1)$, where $h_{tr}(x_1) = \sum_i h_i(x_i)$, the rejection method can be used. As h_{tr} is a mixture of known probability distribution functions, it is possible to generate a random variate X_1 with density proportional to h_{tr}. The weights of the contributions of h_1, h_2 and h_3+h_4 to h_{tr} are obtained by integration over $x \geq a_1$:

$$p_1 = \int_{a_1}^{\infty} h_1(x)dx = \sqrt{\frac{D_1 t}{\pi x_0^2}}. \quad (21a)$$

$$p_2 = \int_{a_1}^{\infty} h_2(x)dx = \sqrt{\frac{D_1 t}{\pi x_0^2}}\, exp\left[-\frac{(x_0-a_1)^2}{4D_1 t}\right]. \quad (21b)$$

$$p_{34} = \int_{a_1}^{\infty} (h_3(x)+h_4(x))dx = \Phi\left(\frac{x_0-a_1}{\sqrt{2D_1 t}}\right) + \mathbf{1}_{[x_0 \leq 2a_1]} \frac{2a_1-x_0}{x_0} \Phi\left(\frac{a_1-x_0}{\sqrt{2D_1 t}}\right). \quad (21c)$$

where $\Phi(z)$ is the normal distribution function:

$$\Phi(z\sqrt{2}) = 1 - Erfc(z)/2. \quad (22)$$

Since h_1 and h_2 are the Rayleigh and tail of Rayleigh distributions [20], the following algorithm (given in the form of a pseudo-code) can be used:

Algorithm 1a
Compute p_1, p_2 and p_{34}. Set $s=p_1+p_2+p_{34}$.
Repeat {
Generate a uniform [0,1] random variate U, V
If $sU \in [0,p_1]$, set $X_1 \leftarrow x_0 + \sqrt{4D_1 tE}$, where E is standard exponential[4].
If $sU \in (p_1, p_1+p_2]$, set $X_1 \leftarrow 2a_1 - x_0 + \sqrt{(x_0-a_1)^2 + 4D_1 tE}$, where E is standard exponential.

[4] A standard exponential random variate is distributed as $p(x)=exp(-x)$, $x \geq 0$. It can be generated from a uniform random number U between 0 and 1 by using $E=-log(U)$.

If $sU \in (p_1+p_2, s]$, let X_1 be a random variate with density proportional to h_3+h_4 (see Alg. 1b below).

} until $Vh_{tr}(X_1) \leq f(X_1)$

Return X_1.

For $x_1 \geq a_1$, we note that $h_4(x_1) \leq h_3^*(2a_1 - x_1)$, where

$$h_3^*(x_1) = \frac{x_0}{x_0\sqrt{4\pi Dt}} \exp\left[-\frac{(x_1 - x_0)^2}{4D_1 t}\right] \times \mathbf{1}_{[x_1 \leq a_1]}. \tag{23}$$

As $h_3 + h_3^*$ is identical to the standard normal density with variance $2D_1t$ centered at x_0, a random variate with density proportional to h_3+h_4 can be generated by using the rejection method:

Algorithm 1b:

Repeat {

Generate N standard normal[5], U uniform on [0,1]

Set $X_1 \leftarrow x_0 + \sqrt{2D_1 t}\mathrm{N}$.

} Until $X_1 > a_1$, or jointly $X_1 < a_1$, $x_0 < 2a_1$ and $U \leq (2X_1 - x_0)/x_0$.

In the former case, return X_1.

In the latter case, return $2a_1 - X_1$.

Algorithm 1a generates pairs (X_1, V) with X_1 having density proportional to h_{tr} and V uniform [0,1] until $Vh_{tr}(X_1) \leq f(X_1)$, and returns X_1. The expected number of iterations is $p_1+p_2+p_{34}$. As it was implicitly shown, $p_{34} \leq 1$ (Eq. 20c), and so the contribution from h_3+h_4 is minor. Algorithm 1b generate random variates X_1 with density proportional to h_3+h_4. The acceptance conditions of this algorithm arise from the inequality $h_4(x_1) \leq h_3^*(2a_1 - x_1)$.

3.1.2 Sampling of the Green's function $p_2(y_1,t|x_0)$

The distribution function to sample in this case is $4\pi y_1^2 p_2(y_1,t|x_0)$. The function $W(u,v)$ can be written as:

$$W(u,v) = \frac{2}{\sqrt{\pi}} \exp(-u^2) R(u+v), \tag{24}$$

---

[5] A standard normal random variate is distributed as $p(x) = (2\pi)^{-1/2} \exp(-x^2/2)$. A normal random variate N can be generated from two random numbers uniformly distributed between 0 and 1 (U_1 and U_2) by using the Box-Muller method, i.e. $\mathrm{N} = \sqrt{-2\ln U_1}\cos(2\pi U_2)$ [19].

where

$$R(x) = \exp(x^2) \int_x^\infty \exp(-t^2)\, dt = M(x\sqrt{2})/\sqrt{2}. \tag{25}$$

M(x) is the classical Mill's ratio, defined as:

$$M(x) = \exp(x^2/2) \int_x^\infty \exp(-t^2/2) dt. \tag{26}$$

The Mill's ratio is monotonically decreasing and convex on the positive half-line. Gordon [22] showed that

$$\frac{x}{x^2+1} \le M(x) \le \frac{1}{x}, \text{ or } \frac{x}{2x^2+1} \le R(x) \le \frac{1}{2x} \tag{27}$$

This property of the Mill's ratio will be exploited to develop a sampling algorithm. We observe that the function to sample ($4\pi\, y_1^2 p_2(y_1, t|\, x_0)$) is proportional to the density:

$$y_1 \left[\frac{\sigma_+ W(\chi_0 + \gamma_1, \sigma_+ \sqrt{t}) - \sigma_- W(\chi_0 + \gamma_1, \sigma_- \sqrt{t})}{\sigma_+ - \sigma_-} \right]. \tag{28}$$

Using eq. (24), and dropping the prefactor $2/\sqrt{\pi}$, the density $f_2(y_1)$ is defined as :

$$f_2(y_1) = y_1 \exp\left[-(y_1 - b + c)^2\right] \left[\frac{\sigma_+ R(y_1 - b + c + \sigma_+ a) - \sigma_- R(y_1 - b + c + \sigma_- a)}{\sigma_+ - \sigma_-} \right], \tag{29}$$

where $a = \sqrt{t}$, $b = a_2/\sqrt{4D_2 t}$, and $c = (x_0 - a_1)/\sqrt{4D_1 t}$. This distribution is not normalized; however, the normalization value is not necessary for the use of the rejection method in this case. Since $\sigma_+ > \sigma_-$, and the Mill's ratio is a monotonically decreasing function, the expression inside the rightmost brackets of eq. (29) leads to the inequality

$$R(y_1 - b + c + \sigma_+ a) + \sigma_- \left[\frac{R(y_1 - b + c + \sigma_+ a) - R(y_1 - b + c + \sigma_- a)}{\sigma_+ - \sigma_-} \right] \le R(y_1 - b + c + \sigma_+ a), \tag{30}$$

This inequality can be used to develop a sampling algorithm. Using the Gordon's upper bound for the Mill's ratio, we can write

$$f_2(y_1) \le \frac{y_1}{2(y_1 - b + c + \sigma_+ a)} \exp\left[-(y_1 - b + c)^2\right]. \tag{31}$$

From this we get the bound

$$f_2(y_1) \le g(y_1) = \frac{1}{2} Max\left(1, \frac{b}{c+\sigma_+ a}\right) \exp\left[-(y_1 - b + c)^2\right]. \quad (32)$$

It is possible to generate a random variate with a density proportional to *g* based on the inequality

$$exp\left[-(x - b + c)^2\right] \le \exp\left[-c^2\right] \times \exp\left[-2(x-b)c\right]. \quad (33)$$

This method is efficient for $c \ge 1$. For $c < 1$, rejection from a normal distribution is used. So the following rejection algorithm to generate a random variate Y_1 with density proportional to f_2:

Algorithm 2: Sampling of a random variate Y_1 with density proportional to f_2

Repeat {
  If $c \ge 1$ {
    Repeat {
      Generate E_1, E_2 standard exponentials
      Set $Y_1 \leftarrow b + E_1/(2c)$
    } Until $(Y_1 - b)^2 < E_2$
  } else {
    Repeat {
      Generate N standard normal
      Set $Y_1 \leftarrow b - c + N/\sqrt{2}$
    } Until $Y_1 \ge b$
  }
  Generate U uniform [0,1]
} Until $Ug(Y_1) \le f_2(Y_1)$
Return Y_1

3.1.3 Sampling of the Green's function $p_3(y_1,t|y_0)$ and $p_4(x_1,t|y_0)$

These Green's functions can be sampled by using the previous algorithms, by interchanging the appropriate parameters and constants in the corresponding Green's functions.

3.2 Brownian dynamics simulation of the ABCD reaction

We set up a BD simulation using the Green's functions derived before using a two-step process: First we determine whether a reaction occurred during the time step Δt. In a second step, the positions of the particles is determined by sampling. At each time step, the state of the pair (AB or CD) is determined by the reaction probabilities $P_{AB \to CD}(\Delta t|x_0)$ and $P_{CD \to AB}(\Delta t|y_0)$ using a uniform random number between 0 and 1 and by comparing it to $P_{AB \to CD}(\Delta t|x_0)$. If the pair initially in the state AB remains in this state, p_1 is

sampled using Algorithm 1. If there is a reaction, p_2 is sampled using Algorithm 2. For a pair initially in the state CD, p_3 or p_4 are sampled depending again on the occurrence of a reaction.

3.3 Look-up table methods

To compare the calculation speed and memory usage of our algorithm with standard look-up tables methods, we have implemented them as in ref. [1]. They are used to generate the interparticle distances X and Y for particles in the state AB and CD respectively. The details are discussed in Appendix B.

3.4 Simulations with the independent reaction times (IRT) method

In a system comprising N particles, the number of pairs of particles is $N(N-1)/2$. Therefore, as each of these pairs can interact, the calculation time for a simulating a system of N particles is approximately proportional to $\sim N^2$. Since a large number of particles is often considered in radiation chemistry simulations, Brownian Dynamics methods usually require a long simulation time, which can be problematic.

To overcome this problem, a method named independent reaction times (IRT) was developed about 30 years ago [23-25]. This method is approximate, but can be used to simulate for radiation chemistry simulations in various conditions of pH and temperature and has been widely used to calculate the radiolytic yields in aqueous solutions [26-29] and in chemical dosimeters [30-31]. This method allows the calculation of radiolytic yields much faster than full step-by-step Brownian Dynamics simulations. However, the positions of the particles at each time step are not calculated; therefore, the extension of the IRT method to problems of interest to radiobiology such as DNA damage simulations may be difficult. In this work, the IRT method is used for comparison with the algorithm presented in this paper. This method is explained in Appendix C.

4. Results and discussion

In the following, we compare Monte Carlo simulation results generated using the algorithms presented in section 3 against the analytical solutions derived in section 2 (section 4.1). We also compare our sampling method to the IRT method (section 4.2), and comment on the asymptotics (section 4.3) and computational performance (section 4.4) of our scheme.

4.1 Green's functions of the ABCD reaction

For the simulation, two particles are initially located at distance $x_0=2.5$, the other parameters being set to $a_1=2$, $D_1=1$, $k_1=5$, $a_2=1$, $D_2=1$, and $k_2=1$. For these parameters, $\tau_1=4$, $k_{D1}=8\pi$, $\mu_1=7/4$, $\tau_2=1$, $k_{D2}=4\pi$, $\mu_2=2$, $\lambda=5$, $\sigma_+=3$, and $\sigma_-=3/4$. In Figure 1a, the analytical Green's functions $4\pi x_1^2 p_1(x_1,t|x_0)$ and $1-4\pi y_1^2 p_2(y_1,t|x_0)$ at t = 0.25, 0.5, 1 and 2 time units are illustrated and compared against the simulation results. These Green's functions represent the probability distribution for the pair to be found in the state AB at distance x_1 or in the state CD at distance y_1 at time t.

Figure 1

The Monte-Carlo results are obtained by using the algorithms described in the Methods section, using 1,000,000 trials. The distances are stored in histograms and normalized. The results for $t=0.25$ are obtained by using the algorithms with single time step. The simulation results are exactly as predicted by the analytical Green's functions. The results for t = 0.5 were obtained by using the Brownian algorithm with two time steps of 0.25, i.e. the interparticle distances of the pairs after the first time step are used as a starting point for the algorithm during the second time step. This is a consequence of the time discretization equation, which allows the simultaneous verification of the algorithms under a wide range of parameters. In fact, similar results are obtained by using any combination of positive time steps for which the sum is 0.5 (results not shown). Obviously, the same observation applies to the simulation at

other time values. We remark that $x \geq a_1$ and $y \geq a_2$, since the inter-particle distance cannot be shorter than their reaction radii.

The survival and reaction probabilities for the pairs in the state AB or CD as a function of time are shown in Figure 1b. The parameters used for this simulations are those of the system presented in Figure 1a. The asymptotic limit, given by

$$P_{AB\to CD}(t \mid x_0) \sim \frac{a_1}{x_0} \frac{k_1 / k_{D_1}}{1 + k_1 / k_{D_1} + k_2 / k_{D_2}} \left(1 - \frac{2\chi_1}{\sqrt{\pi}} + \frac{\sqrt{\tau_2} - 1/\sigma_+ - 1/\sigma_-}{\sqrt{\pi t}} \right), \tag{34}$$

is also plotted.

4.2 Comparison with the IRT method.

The IRT method has been validated by many approaches [27,28]. In a recent paper, we compared the IRT simulation results with the GFDE for a reaction of type ABC [18]. In the present work, we compare the results obtained by the two methods for the reaction ABCD.

Figure 2

In Figure 2, we show the time evolution of the state of a pair of particles AB initially at position $x_0=2.5$, using the parameters $a_1=2$, $D_1=1$, $k_1=5$, $a_2=1$, $D_2=1$ and three values of k_2 ($k_2=0$, $k_2=1$ and $k_2=10$), as simulated by our algorithms and by the IRT method. In all cases, the agreement between the results from the IRT method and the Green's function is excellent. As expected, the survival probability in the AB form increases with increasing k_2. It is important to note here that the distance at which the products are placed following a chemical reaction plays a critical role. If the products are not placed at distance a_2 after a reaction AB→CD, the results provided by IRT do not match the analytical Green's functions (results not shown), because the boundary condition of the GFDE states that the number of reactions AB occurring at the reaction radius a_1 are equal to number of times that products CD are formed at the reaction radius a_2. This property is necessary for material balance. The asymptotics (Eq. 36) are also plotted in Figure 2.

4.3. Transition

The long-time asymptotic behavior of the survival probabilities is, in general, $\sim t^{-1/2}$ according to Eq. (36). As discussed by Popov and Agmon [10], the asymptotic limit is approached from above if

$$\left(1+\frac{k_1}{k_{D_1}}+\frac{k_2}{k_{D_2}}\right)\frac{x_0}{a_1}<\frac{k_2}{k_{D_2}}\sqrt{\frac{\tau_2}{\tau_1}}+\frac{k_1}{k_{D_1}}. \tag{35}$$

and from below in the opposite case. At the transition, i.e. when the right and left sides of eq. 35 are equal, the long time asymptotic behavior is $\sim t^{-3/2}$. We wanted to see if this transition can be observed from the Brownian Dynamics simulations and the IRT method.

We have performed simulations using the Brownian Dynamics described in this paper, as well as by the IRT method, using the parameters $a_1=1$, $k_1=5$, $a_2=4$, $D_2=1$, $k_2=8$ and $x_0=1.625$, for $D_1=0.5$, $D_1=1.0$ and $D_1=1.5$. The ratio and difference between $P_{AB\rightarrow CD}(\Delta t|x_0)$ and $P_{AB\rightarrow CD}(\Delta t|\infty)$ are shown in Figure 3.

Figure 3

For the system considered, a transition occurs for $D_1=1$. For $D_1>1$, the probability decreases monotonically, whereas for $D_1<1$, there is a maximum, which appears in Figure 3a. The results are also in good agreement with those obtained by the IRT method. At the transition, the long time asymptotic behavior is $\sim t^{-3/2}$. To illustrate this dependence, the data shown in Figure 3a are presented on a log-log scale in Figure 3b. The slopes of the reaction probabilities follow their respective $\sim t^{-1/2}$ and $\sim t^{-3/2}$ behavior, as indicated by the straight lines. However, the IRT results are different from the predicted curves on this scale, at least at large time values. The reason for this difference is not clear. We have tried to increase the number of trials and the precision of the numbers, but there was no improvement in the results. The difference is probably inherent to the IRT method itself. Additionally, as only forward reactions are considered, there is no such transition in forward reaction probabilities used in the IRT method.

Nevertheless, the IRT method is used for the short time scale of radiation chemistry, and the overall difference with the predicted results remains small.

4.4 Performance and limitation of the algorithms

Usually, table look-up methods are used to generate samples from the GFDE in Brownian Dynamics simulations [1, 7, 32-33].We have studied the performance (Table 1), precision (Table 2) and memory requirements (Table 3) of our algorithm and table look-up methods. In Table 1, we compare the time needed for our algorithm and look-up tables for a time step of 0.1, 0.5, 1, 5 and 10 units, in the same simulation conditions ($x_0=2.5$, $a_2=1$, $D_1=1$, $k_1=5$, $a_2=1$, $D_2=1$ and $k_2=1$). The simulations are performed using an Intel Xeon CPU E5430 @ 2.66 GHz. Our algorithm is in general faster than the look-up tables, but the simulation time for our algorithm increases with t. This may be due to the fact that the number of iterations of Algorithm 1 is $p_1+p_2+p_{34}$, and p_1 and p_2 are both proportional to $\sqrt{t}$ (see section 3.1.1). For the look-up table method, the simulation time essentially only depends on the size of the table, as expected.

Table 1

A χ^2 test is performed using 10,000, 100,000 and 1,000,000 histories to evaluate if the sampled distribution is different from the analytical predictions. The critical value of the χ^2 test for 178 degrees of freedom is ~210, using a probability value of 0.05. Therefore, a χ^2 value below the critical value indicates that the distributions are not significantly different.

Table 2

In Table 2, χ^2 values are shown for our algorithm and for the table look-up methods. For our algorithm, the values are all <210, indicating that the distributions are not statistically different. For table look-up

methods, many χ^2 values are higher than this threshold, especially for tables with 500 and 1,000 bins. Although the χ^2 test is quite strict[6] these results indicate that a resolution of at least 2,000 bins may be necessary for the tables. The apparent decrease of accuracy when the time increases is probably due to the fact that at short times, the functions are peaked, meaning that many points used for the comparison as well as the GFDE are 0. Since they are counted as 0 they don't contribute to the χ^2 values. Obviously this in no longer the case when time increases, since the functions become flatter and more values are different from 0.

The memory usage of the algorithms is done by counting the number of bytes needed by each variables used. Since our algorithm does not require storing of more than a few variables, the memory requirement doesn't exceed 12 kB, as indicated by the Windows Task Manager. For table methods, the tables for p_1, p_2, p_3 and p_4 are calculated for 200 different values of x_0 or y_0; therefore, the memory requirement increases with the number of bins. The memory usage is in agreement with the fact that a double precision number occupies 8 bits in memory. For example, for the tables with 500 bins, the memory requirement is 4×500×200×8 bytes = 3,125 kB (1kB = 1,024 bytes).

Table 3

4.5 Applicability of the simulation methods

[6] The χ^2 test has its limitations for comparing distributions, especially when the expected frequency is low, which happens at the tails of the Green's functions for small t values. Despite its limitations, we decided to use it because it is well known and relatively easy to use. In this work, our algorithms are exact and therefore the distribution of the sampled values should not be statistically different from the predicted values.

The Green's functions used here are exact only for systems comprising two particles. The problem becomes much more complex when more than two particles are involved and the Green's functions are no longer exact. If more than two particles are close to each other, the Green's function can be obtained numerically, and table look-up methods can be used [33]. If particles are too far from each other, the particles do not interact and therefore it is not necessary to sample the propagator of the inter-particle distance distribution. The decision to use the sampling algorithm (or not) is often based on the "reaction zone", which is defined near each particle. The condition $r_0<[R+8(2Dt)^{1/2}]$ is used in ref. [32] and many others to define the reaction zone. It should also be noted that in the IRT method, there is be competition between reactions, so that the equations presented in this paper can be strongly incorrect in systems comprising more than two particles.

If there is an electrostatic interaction between the particles, e.g. a Coulomb potential, it is necessary to use the Green's functions of the Debye-Smoluchowski equation [34]. In the reactions occurring during the radiolysis of water [11], most reactions of type ABCD involve charged particles on at least one side of the reaction. However, the Green's functions for the ABC and ABCD reactions cover a large number of chemical reactions occurring in biological systems. They can also be useful to validate the Green's functions of the Debye-Smoluchowski equation, since they should be equal when there is no electric field present.

5. Conclusion

The GFDE are used in many particle-based chemical simulations codes. The sampling of the Brownian propagators is therefore of great interest for such codes. The GFDE for the ABCD reactions are quite complex; however, it is possible to use the relatively simple algorithms presented in this paper to simulate the evolution in time and space of pairs of particles. In general, the performance of our algorithm is similar or better than that of table methods. Table methods usually necessitate an extensive set-up to calculate and hold the pre-calculated data, which may be very time and memory consuming, especially when the

table has more than one dimension [33] and, as it will be the case in our future work, when large systems comprising many types of particles with different reaction channels are simulated.

This method might be useful for particle-based event-driven simulation schemes of the FPKMC (first-passage kinetic Monte-Carlo) [13] and GFRD (Green's functions reaction dynamics) [8]. For example, in the GFRD method, simple geometric domains such as spheres are put around at most two particles to shield them from the influence of other particles. The pairs of particles are then propagated locally in an exact manner by basically sampling times and associated positions up to the time up to which any other particle outside the domain is guaranteed not to enter it. By propagating the domains subsequently, an event-driven particle-based simulation can be set up that is both exact and efficient, using exact Green's functions in order to skip other diffusion events. Such a scheme naturally gets rid of the problems associated with the possible interference of other particles at long times. One of the still pending problems of GFRD-like methods is the lack of Green's functions that correctly incorporate the back-reaction; for that reason, product particles that dissociate have to be put in contact (from where they reacted), which diminishes the performance of the scheme. This scheme would highly benefit from having exact Green's functions and associated sampling prescriptions that incorporate both the forward and backward reaction, such as the one described in the paper.

In radiation chemistry, the IRT method has been used to calculate the yields of the radiolytic species in solutions [25-29] and also in chemical dosimeters [30-31]. The IRT method is based on the survival probability of the pairs of particles in the system, and the competition between reactions are taken into consideration by sorting the sampled reaction time. Although the purpose of this article is not the validation of the IRT method, it is interesting to note that our simulation results are in excellent agreement with those predicted by IRT. In fact, to our knowledge, the comparison of the predictions of the analytical Green's functions with the IRT results for 2-particle systems with reversible diffusion-influenced reactions has not been done before. Even if the simulation results obtained by the IRT method fail to yield the proper asymptotic long time dependence, the agreement with the GFDE is excellent at short times, which is of interest for radiation chemistry codes.

Because the algorithms are simple and use only a few kilobytes of memory, they can probably be used on a general-purpose graphic processing unit (GPGPU). A GPGPU is a computing device operating as a co-processor to the main central processing unit (CPU). GPGPUs comprise up to several hundred cores and have their own memory. They are used to compute functions which are executed a large number of times, but independently on different data. Therefore, the algorithms could be implemented on a GPGPU to simulate a chemical system comprising different types of particles. This work should be useful for chemistry codes that are based on this approach to study biochemical interactions occurring in cells, which may eventually be included in event-based models of space radiation risks.

Acknowledgements

We would like to thank the reviewers for their careful review. This work was supported by the National Aeronautics and Space Administration (NASA) contract number NAS9-02078.

References

[1] A.V. Popov, N. Agmon, Three-dimensional simulations of reversible bimolecular reactions. III. The pseudo-unimolecular ABCD reaction. J. Chem. Phys. 118 (2003) 11057-11065. doi: 10.1063/1.1570816

[2] A.L. Edelstein, N. Agmon, Equilibration in reversible bimolecular reactions, J. Phys. Chem. 99 (1995) 5389-5401. doi: 10.1021/j100015a024

[3] N. Agmon, Diffusion with back reaction. J. Chem. Phys 81 (1984) 2811-2817. doi: 10.1063/1.447954

[4] H. Kim, K.J. Shin, N. Agmon, Excited-state reversible geminate recombination with quenching in one dimension, J. Chem. Phys. 111 (1999) 3791-3799. doi: 10.1063/1.479682

[5] N. Agmon, A.V. Popov, Unified theory of reversible target reactions, J. Chem. Phys. 119 (2003) 6680-6690. doi: 10.1063/1.1603717

[6] H. Kim, K.J. Shin, Exact solution of the reversible diffusion-influenced reaction for an isolated pair in three dimensions, Phys. Rev. Lett. 82 (1999) 1578-1581. doi: 10.1103/PhysRevLett.82.1578

[7] S. Park, N. Agmon, Theory and simulation of diffusion-controlled Michaelis−Menten kinetics for a static enzyme in solution, J. Phys. Chem. B 112 (2008) 5977-5987. doi: 10.1021/jp075941d

[8] J.S. van Zon, P.R. ten Wolde, Green's function reaction dynamics: A particle-based approach for simulating biochemical networks in time and space, J. Chem. Phys. 123 (2005) 234910. doi: 10.1063/1.2137716

[9] H. Kim, K.J. Shin, N, Agmon, Diffusion-influenced reversible geminate recombination in one dimension. II. Effect of a constant field. J. Chem. Phys. 114 (2001) 3905-3912. doi: 10.1063/1.1344607

[10] A.V. Popov, N. Agmon, Exact solution for the geminate ABCD reaction, J. Chem. Phys. 117 (2002) 5770-5779. doi: 10.1063/1.1501127

[11] K. Takahashi, S. Tănase-Nicola, P.R. ten Wolde, Spatio-temporal correlations can drastically change the response of a MAPK pathway. PNAS 107 (2010) 2473-2478. doi: 10.1073/pnas.0906885107

[12] K. Schwarz, H. Rieger, Efficient kinetic Monte Carlo method for reaction–diffusion problems with spatially varying annihilation rates. J. Comput. Phys. 237 (2013) 396-410. doi: doi:10.1016/j.jcp.2012.11.036

[13] A. J. Mauro, J. K. Sigurdsson, J. Shrake, P.J. Atzberger, S.A. Isaacson. A First-Passage Kinetic Monte Carlo method for reaction–drift–diffusion processes. J. Comput. Phys. 259 (2014) 536-567. doi: 10.1016/j.jcp.2013.12.023

[14] I. Plante, A Monte-Carlo step-by-step simulation code of the non-homogeneous chemistry of the radiolysis of water and aqueous solutions. Part I: theoretical framework and implementation, Radiat. Env. Biophys. 50 (2011) 389-403. doi: 10.1007/s00411-011-0367-8

[15] I. Plante, A Monte-Carlo step-by-step simulation code of the non-homogeneous chemistry of the radiolysis of water and aqueous solutions. Part II: Calculation of radiolytic yields under different conditions of LET, pH and temperature, Radiat. Env. Biophys. 50 (2011) 389-403. doi: 10.1007/s00411-011-0368-7

[16] I. Plante, T. Tippayamontri, N. Autsavapromporn, J. Meesungnoen, J.-P. Jay-Gerin, Monte-Carlo simulation of the radiolysis of the ceric sulfate dosimeter by low-LET radiation, Can. J. Chem. 90 (2012) 717-723. doi: 10.1139/v2012-052

[17] I. Plante, F.A. Cucinotta, Model of the initiation of signal transduction by ligands in a cell culture: Simulation of molecules near a plane membrane comprising receptors, Phys. Rev. E. 84 (2011), 051920. doi: 10.1103/PhysRevE.84.051920

[18] I. Plante, L. Devroye, F.A. Cucinotta, Random sampling of the Green's functions for reversible reactions with an intermediate state. J. Comput. Phys. 242 (2013) 531-543. doi: 10.1016/j.jcp.2013.02.001

[19] W.H. Press, S.A. Teukolsky, W.T. Vetterling, B.P. Flannery, Numerical Recipes in C, 2nd Edition, Cambridge University Press, Cambridge, 1992.

[20] L. Devroye, Non-Uniform Variate Generation, Springer-Verlag, New York, 1986. luc.devroye.org/rnbookindex.html

[21] J. von Neumann, Monte Carlo Method, National Bureau of Standards Series, vol. 12, pp. 36-38, 1951.

[22] R. Gordon, Values of Mills ratio of area to bounding ordinate and of the normal probability integral for large values of the argument. An. Math. Stat. 12 (1941) 364-366.

[23] N.J.B. Green, M.J. Pilling, S.M. Pimblott, P. Clifford, Stochastic modeling of fast kinetics in a radiation track, J. Phys. Chem. 94 (1990) 251-258. doi: 10.1021/j100364a041

[24] P. Clifford, N.J.B. Green, M.J. Pilling, Stochastic model based on pair distribution functions for reaction in a radiation-induced spur containing one type of radical, J. Phys. Chem. 86 (1982) 1318-1321. doi: 10.1021/j100397a021

[25] P. Clifford, N.J.B. Green, M. Oldfield, M.J. Pilling, S.M. Pimblott, Stochastic models of multi-species kinetics in radiation-induced spurs, J. Chem. Soc., Faraday Trans. 1 82 (1986) 2673-2689. doi:10.1039/f19868202673

[26] S.M. Pimblott, J.A. LaVerne. Stochastic simulation of the electron radiolysis of water and aqueous solutions. J. Phys. Chem. A 101 (1997) 5828-5838. doi: 10.1021/jp970637d

[27] T. Goulet, M.-J. Fraser, Y. Frongillo, J.-P. Jay-Gerin. On the validity of the Independent Reaction Times approximation for the description of the nonhomogeneous kinetics of liquid water radiolysis. Radiat. Phys. Chem. 51 (1998) 85-91. doi: 10.1016/S0969-806X(97)00060-1

[28] Y. Frongillo, T. Goulet, M.-J. Fraser, V. Cobut, J.P. Patau, J.-P. Jay-Gerin, Monte Carlo simulation of fast electron and proton tracks in liquid water - II. Nonhomogeneous chemistry, Radiat. Phys. Chem. 51 (1998) 245-254. doi: 10.1016/S0969-806X(97)00097-2

[29] J. Meesungnoen, J.-P. Jay-Gerin, High-LET radiolysis of liquid water with $^{1}H^{+}$, $^{4}He^{2+}$, $^{12}C^{6+}$, and $^{20}Ne^{9+}$ ions: Effects of multiple ionization, J. Phys. Chem. A 109 (2005) 6406-6419. doi: 10.1021/jp058037z

[30] N. Autsavapromporn, J. Meesungnoen, I. Plante, J.-P. Jay-Gerin, Monte Carlo simulation study of the effects of acidity and LET on the primary free-radical and molecular yields of water radiolysis – Application to the Fricke Dosimeter, Can. J. Chem. 85 (2007) 214-229. doi: 10.1139/V07-021

[31] R. Meesat, S. Sanguanmith, J. Meesungnoen, M. Lepage, A. Khalil, J.P. Jay-Gerin, Utilization of the ferrous sulfate (Fricke) dosimeter for evaluating the radioprotective potential of cystamine: Experiment and Monte Carlo simulation. Radiat. Res. 177 (2012) 813-826. doi: 10.1667/RR2829.1

[32] A.V. Popov, N. Agmon, Three-dimensional simulations of reversible bimolecular reactions: the simple target problem, J. Chem. Phys. 115 (2001) 8921-8932. doi: 10.1063/1.1412609

[33] S. Park, K.J. Shin, A.V. Popov, N. Agmon, Diffusion-influenced excited-state transfer reactions, A*+B↔C*+D, with two different lifetimes: Theories and simulations, J. Chem. Phys. 123 (2005) 034507. doi: 10.1063/1.1948369

[34] K.M. Hong, J. Noolandi, Solution of the Smoluchowski equation with a Coulomb potential. I. General results, J. Chem. Phys 68 (1978) 5163-5171. doi:10.1063/1.435636

Appendix A: Time discretization equations

A simulation is usually divided in a finite number of time steps. However, the final distribution of inter-particle distributions of distances and states of particles should depend only of the sum of the time steps. This property can be expressed mathematically by Chapman-Kolmogorov type equations, which hold for Markovian systems. As discussed in previous work [11,17-18], these equations offer a way to validate the algorithms presented in this paper. In this Appendix, six equations of this type will be established. If the time t is the sum of two time steps $t=t_1+t_2$, a pair of particles in the state AB initially separated by distance x_0 that is found at distance x_2 at time t_1+t_2 can i) Go to the distance x_1 during t_1 and go to its final distance x_2 during t_2, or ii) React to the state CD at distance y_1 during t_1 and then react to the state AB to distance x_2 during t_2. Hence, the Green's functions are linked as follow:

$$p_1(x_2,t_1+t_2 \mid x_0) = \int_{a_1}^{\infty} p_1(x_2,t_2 \mid x_1)p_1(x_1,t_1 \mid x_0)4\pi x_1^2 dx_1 + \int_{a_2}^{\infty} p_4(x_2,t_2 \mid y_1)p_2(y_1,t_1 \mid x_0)4\pi y_1^2 dy_1 . \quad \text{(A1)}$$

Similarly, a pair of particles initially in the state AB at distance x_0 that is found later in the state CD at distance y_2 at time $t_1+ t_2$ can: i) Move to x_1 during t_1 and react to the state CD to distance y_2 during t_2, or ii) React to the state CD at distance y_1 during t_1 and move to y_2 during t_2. This leads to the following equation:

$$p_2(y_2,t_1+t_2 \mid x_0) = \int_{a_1}^{\infty} p_2(y_2,t_2 \mid x_1)p_1(x_1,t_1 \mid x_0)4\pi x_1^2 dx_1 + \int_{a_2}^{\infty} p_3(y_2,t_2 \mid y_1)p_2(y_1,t_1 \mid x_0)4\pi y_1^2 dy_1 . \quad \text{(A2)}$$

Using the same approach for pairs initially in the state CD at initial distance y_0, time discretization for p_3 and p_4 can be obtained:

$$p_3(y_2,t_1+t_2 \mid y_0) = \int_{a_2}^{\infty} p_3(y_2,t_2 \mid y_1)p_3(y_1,t_1 \mid y_0)4\pi y_1^2 dy_1 + \int_{a_1}^{\infty} p_2(y_2,t_2 \mid x_1)p_4(y_1,t_1 \mid y_0)4\pi x_1^2 dx_1 , \quad \text{(A3)}$$

$$p_4(x_2,t_1+t_2 \mid y_0) = \int_{a_2}^{\infty} p_4(x_2,t_2 \mid y_1)p_3(y_1,t_1 \mid x_0)4\pi y_1^2 dy_1 + \int_{a_1}^{\infty} p_1(x_2,t_2 \mid x_1)p_4(x_1,t_1 \mid y_0)4\pi x_1^2 dx_1 . \quad \text{(A4)}$$

The time discretization equations can also be established for the probabilities of reaction.

$$P_{AB\to CD}(t_1+t_2\mid x_0)=\int_{a_1}^{\infty}P_{AB\to CD}(t_2\mid x_1)p_1(x_1,t_1\mid x_0)4\pi x_1^2dx_1+\int_{a_2}^{\infty}(1-P_{CD\to AB}(t_2\mid y_1))p_2(y_1,t_1\mid x_0)4\pi y_1^2dy_1\ , \quad \text{(A5)}$$

$$P_{CD\to AB}(t_1+t_2\mid y_0)=\int_{a_2}^{\infty}P_{CD\to AB}(t_2\mid y_1)p_3(y_1,t_1\mid y_0)4\pi y_1^2dy_1+\int_{a_1}^{\infty}(1-P_{AB\to CD}(t_2\mid x_1))p_4(x_1,t_1\mid y_0)4\pi x_1^2dx_1$$

. (A6)

It was not possible to formally prove eqs. A1-A6 directly by using the analytic expressions of the Green's functions in the integrals, but we are able to prove them indirectly by showing that they are solutions of their respective diffusion equation and boundary conditions (see supporting document 1). In addition, eqs A1-A6 are verified numerically for different values of x_0, x_2, y_0, y_2, k_1, k_2, a_1, a_2, D_1, D_2, Δt_1, and Δt_2 (see supporting Mathematica document).

Appendix B: Look-up table methods

The look-up table method is the standard technique used to generate random values of the interparticle distances X and Y. A brief description is provided here.

A random number U uniformly distributed between 0 and 1 is generated. For a pair in the AB state initially at distance x_0, if $< \int_{a_1}^{\infty} 4\pi x_1^2 p_1(x_1, t|x_0) dx_1$, the system remains in the AB state at time t. The sampled value X is determined from the equation

$$U = \int_{a_1}^{X} 4\pi x_1^2 p_1(x_1, t \mid x_0) dx_1 \,. \tag{B1}$$

On the other hand, if $U \geq \int_{a_1}^{\infty} 4\pi x_1^2 p_1(x_1, t|x_0) dx_1$, the system has reacted to the CD state. In this case, the value of Y is found by using

$$U = \int_{a_1}^{\infty} 4\pi x_1^2 p_1(x_1, t \mid x_0) dx_1 + \int_{a_2}^{Y} 4\pi y_1^2 p_2(y_1, t \mid x_0) dx_1 \,. \tag{B2}$$

The integrals can be calculated analytically or numerically. However, their analytical forms are too complicated to be inverted to find X or Y. Therefore, it is necessary to pre-calculate the tables for an array of values of X and Y. The closest value is found by using a binary search algorithm within the array. To improve the precision, an interpolation is performed. For a fixed value of t, and considering that the parameters a_1, D_1, k_1, a_2, D_2 and k_2 are also fixed for one simulation, the tables are still dependent on the initial value x_0, and needs to be calculated for several values of x_0.

Appendix C: The independent reaction times (IRT) method

A detailed description of the IRT method is beyond the scope of this paper; therefore, only the most important points will be given here. Briefly, knowing the initial positions of the particles in the system, a reaction time is sampled for each pair of particles by solving the equation numerically

$$\frac{R\alpha+1}{r_0\alpha}\left[W\left(\frac{r_0-R}{\sqrt{4Dt}},\alpha\sqrt{Dt}\right)-Erfc\left(\frac{r_0-R}{\sqrt{4Dt}}\right)\right]=U\,, \tag{C1}$$

for t, where r_0 is the initial distance between pairs, R is the reaction radius, $\alpha=-(1+k_i/k_{Di})/R$, and U is a random number uniformly distributed between 0 and 1. If the time value given by eq. C1 is infinite, it indicates that a reaction is not possible. Similarly, a reaction time can be obtained for first-order processes (not present in this actual work) by sampling an exponential distribution with parameter given by the inverse of the dissociation rate constant. The reaction times are sorted and the reactions are processed according to the time in the list, by deleting reactants and adding reaction products at positions are that are determined by the position approach described in Clifford et al. [25]. The reaction time list is updated after each reaction. It can be mentioned here that in some implementations of IRT, the position of the non-reacted species may be updated by simple 3D diffusion. However, it is not the case for this work. The reactions are done until the final time is reached. With this method, the competition between reactions is described via sorting the reaction times [27].

Tables

Table 1. Average calculation times (s) for 1,000,000 simulation histories ($x_0=2.5$, $a_2=1$, $D_1=1$, $k_1=5$, $a_2=1$, $D_2=1$ and $k_2=1$)

Time step	0.1	0.5	1	5	10
Our algorithm	3.6	4.0	5.0	13.4	23.8
Table look-up					
500 bins	8.1	8.3	8.2	8.2	8.1
1,000 bins	25.1	24.9	25.0	25.0	25.0
2,000 bins	42.5	42.7	42.1	42.3	42.7
5,000 bins	104.5	105.3	105.8	104.7	105.0

Table 2. Maximum χ^2 values for the simulations ($x_0=2.5$, $a_2=1$, $D_1=1$, $k_1=5$, $a_2=1$, $D_2=1$ and $k_2=1$)

Time step	0.1	0.5	1	5	10
Our algorithm	48.5	54.6	90.9	199.6	193.9
Table look-up					
500 bins	190.7	547.1	287.4	251.3	212.7
1,000 bins	80.3	106.3	103.7	164.1	212.2
2,000 bins	92.4	49.3	80.7	183.3	221.3
5,000 bins	83.1	64.3	116.2	177.4	163.8

Table 3. Memory usage

	Our algorithm	Table look-up (500 bins)	Table look-up (1,000 bins)	Table look-up (2,000 bins)	Table look-up (5,000 bins)
Memory usage	~12 kB	~3,136 kB	~6,336 kB	~12,520 kB	~31,308 kB

Figure captions

Figure 1: a) Green's functions $4\pi r^2 p_1(x,t|x_0)$ (bottom) and $1-4\pi y^2 p_2(y,t|x_0)$ (top) for $x_0=2.5$, $a_2=1$, $D_1=1$, $k_1=5$, $a_2=1$, $D_2=1$ and $k_2=1$, at 0.25, 0.5, 1 and 2 time units. Analytical functions: (—); result of sampling: (■). b) Fraction of particles in the state AB ($1-P_{AB\to CD}(\Delta t|x_0)$) and in the state CD ($P_{AB\to CD}(\Delta t|x_0)$). The time is in arbitrary units.

Figure 2: Probability of the particles to be in the state AB (top) or CD (bottom), assuming that all particles are initially in the state AB at distance $x_0=2.5$. The parameters are $a_2=1$, $D_1=1$, $k_1=5$, $a_2=1$, $D_2=1$. The curves are plotted for $k_2=0$, $k_2=1$ and $k_2=10$. Analytical functions: (—); asymptotics: (---); results from IRT simulation: (■).

Figure 3: Ratio $P_{AB\to CD}(t|x_0)/P_{AB\to CD}(\infty|x_0)$ (a) and difference $P_{AB\to CD}(t|x_0)-P_{AB\to CD}(\infty|x_0)$ (b) of the reaction probabilities for a pair initially in the state AB, with the parameters $a_1=1$, $k_1=5$, $a_2=4$, $D_2=1$, $k_2=8$, $x_0=1.625$, for $D_1=0.5$, $D_1=1.0$ (transition) and $D_1=1.5$. Simulations performed with the IRT methods (dots) are shown as well.

Figure 1

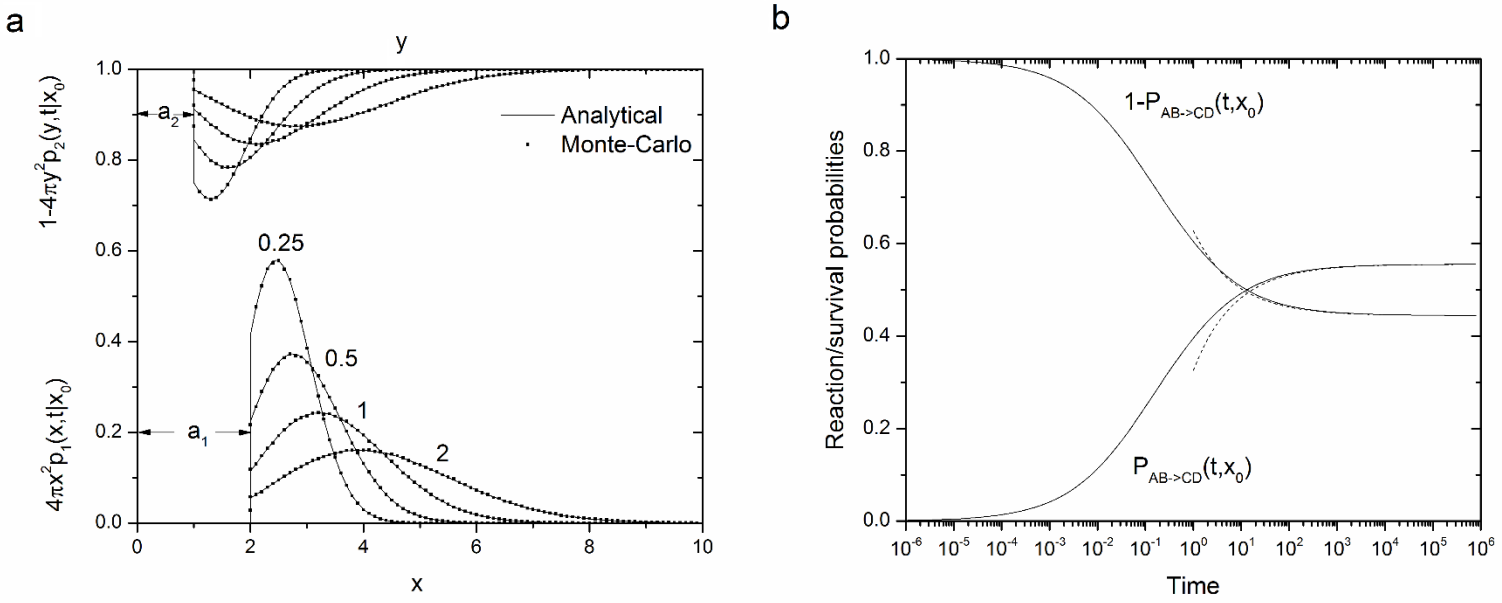
a
b
y
x
Analytical
Monte-Carlo
0.25
0.5
1
2
a_1
a_2
$1-4\pi y^2 p_2(y,t|x_0)$
$4\pi x^2 p_1(x,t|x_0)$
Reaction/survival probabilities
Time
$1-P_{AB->CD}(t,x_0)$
$P_{AB->CD}(t,x_0)$

Figure 2

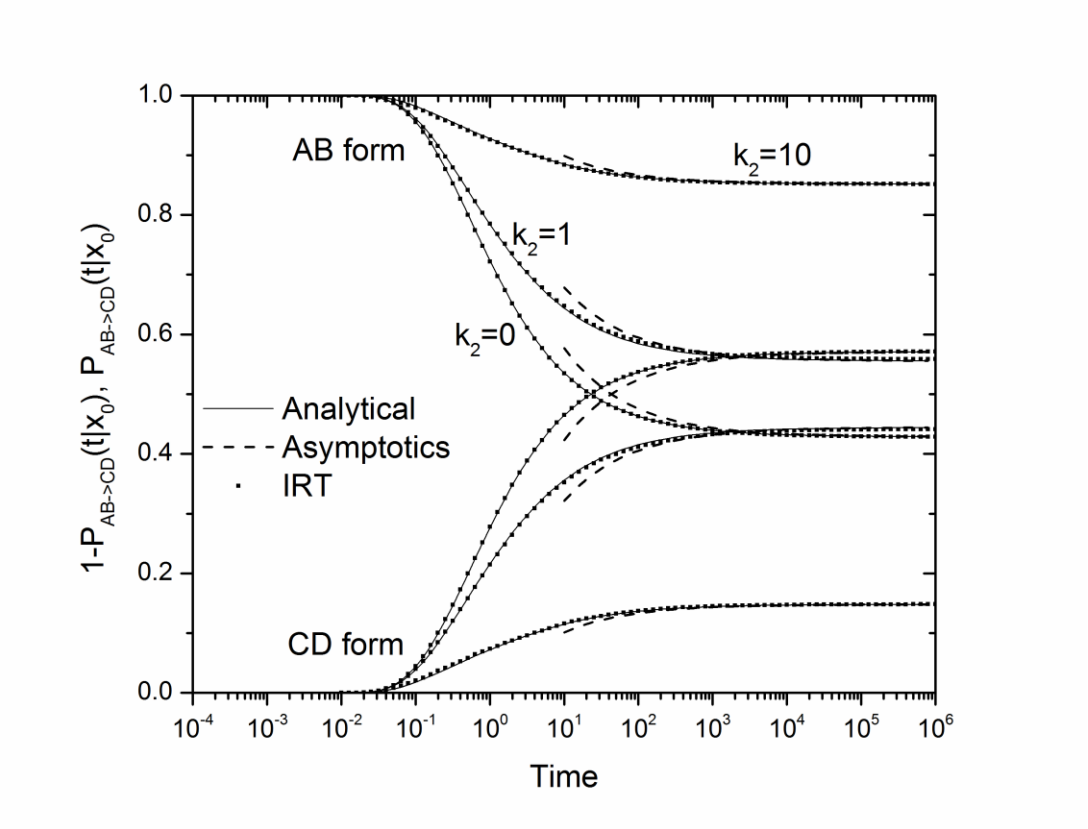
1.0
0.8
0.6
0.4
0.2
0.0
AB form
k_2=10
k_2=1
k_2=0
Analytical
Asymptotics
IRT
CD form
$1-P_{AB->CD}(t|x_0)$, $P_{AB->CD}(t|x_0)$
10^{-4} 10^{-3} 10^{-2} 10^{-1} 10^{0} 10^{1} 10^{2} 10^{3} 10^{4} 10^{5} 10^{6}
Time

Figure 3

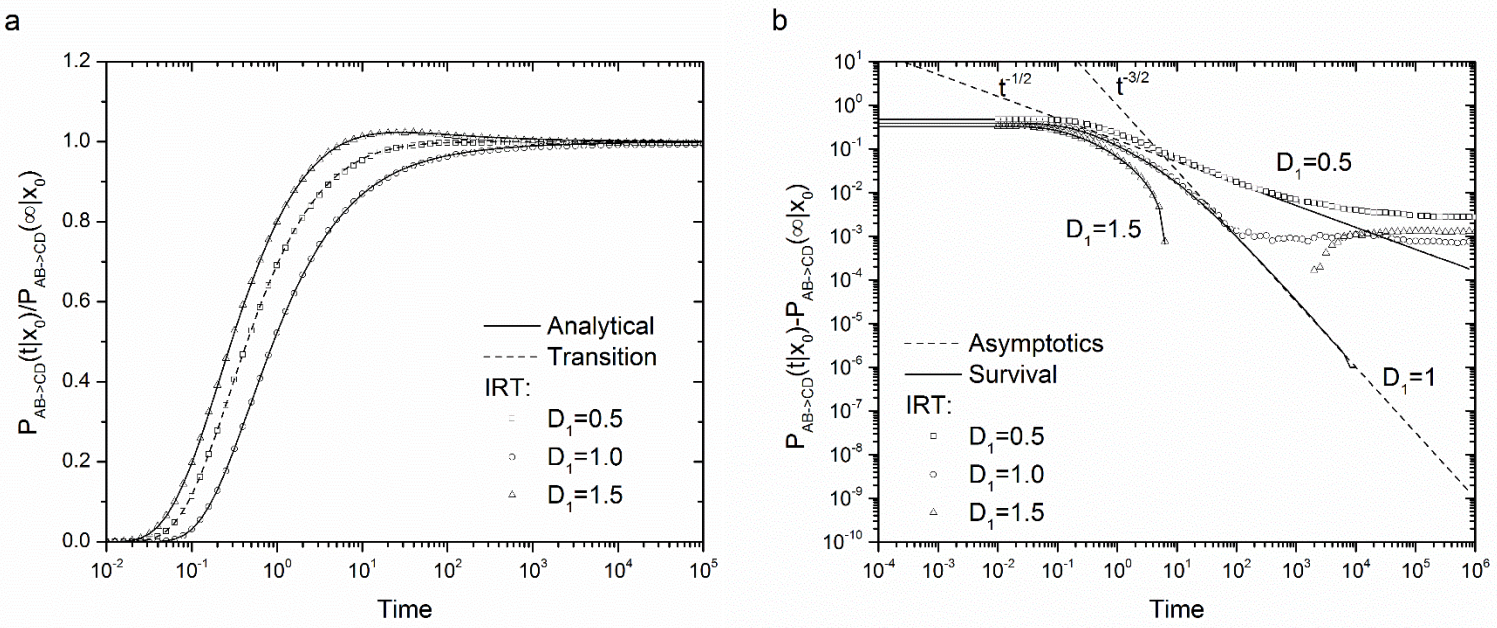
a
b
Analytical
Transition
IRT:
D1=0.5
D1=1.0
D1=1.5
Time
t-1/2
t-3/2
D1=0.5
D1=1.5
D1=1
Asymptotics
Survival
IRT:
D1=0.5
D1=1.0
D1=1.5
Time